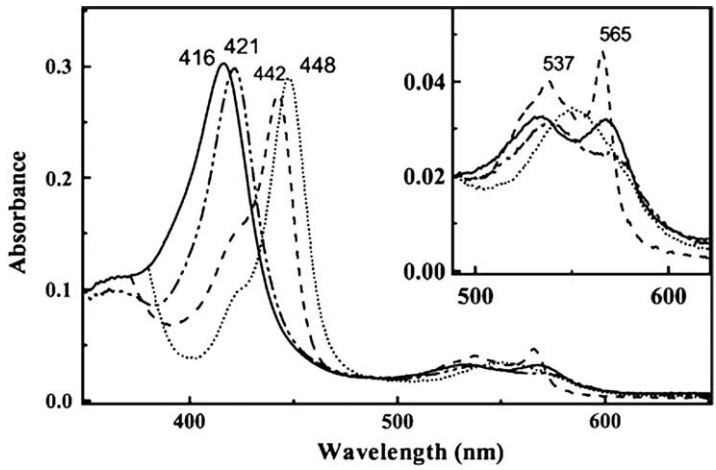

Figure 13.7 Spectral changes induced by ritonavir in CYP3A4. Absorbance spectra of ferric ligand-free (—), ferric ritonavir-bound (–···–), ferrous ritonavir-bound (- - -) and ferrous-CO adduct (····) of 3 μM CYP3A4 were recorded in buffer (50 mM phosphate, pH 7.5, 20% glycerol, and 1 mM dithiothreitol).

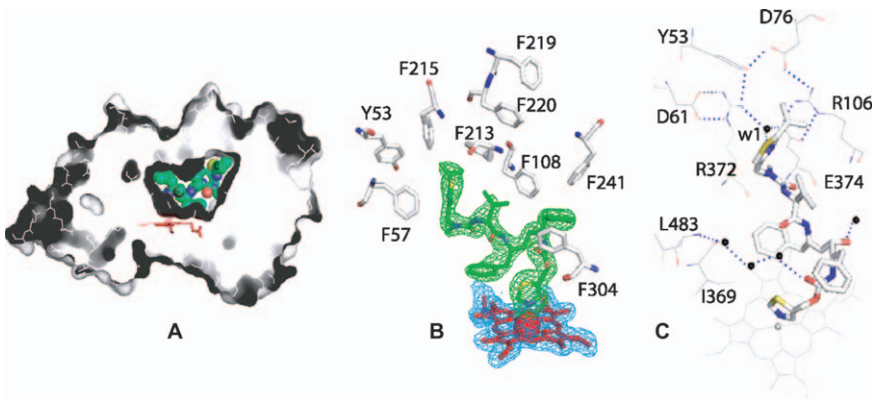

Figure 13.8 Crystal structure of the CYP3A4-ritonavir complex. (A) The active site cavity of ritonavir-bound CYP3A4. Ritonavir is green and in CPK representation; the heme is red. (B) Aromatic residues surrounding ritonavir. $2F_o - F_c$ (blue) and $F_o - F_c$ (green) electron density maps around the heme and ritonavir are contoured at 1σ and 3σ, respectively. (C) An umbrella-like charge–charge/H-bonding network connected to the isopropylthiazole moiety of ritonavir *via* a highly ordered water molecule (w1) (2.0 Å).

CYP3A inhibitors, reflecting the importance of the 5-thiazolyl moiety. These structure–activity relationship data suggest that the high CYP3A-inhibitory potency associated with ritonavir is due both to hydrophobic interactions with CYP3A and the direct ligation of the heme iron by the thiazole moieties.